



Morphological integration and modularity in the hyperkinetic feeding system of aquatic-foraging snakes

Daniel Rhoda,^{1,2} P. David Polly,³ Christopher Raxworthy,¹ and Marion Segall^{1,4}

¹Department of Herpetology, American Museum of Natural History, New York, New York 10024

²Committee on Evolutionary Biology, University of Chicago, Chicago, Illinois 60637

³Department of Geological Sciences, Indiana University, Bloomington, Indiana 47405

⁴E-mail: marion.segall@live.fr

Received September 11, 2020

Accepted November 13, 2020

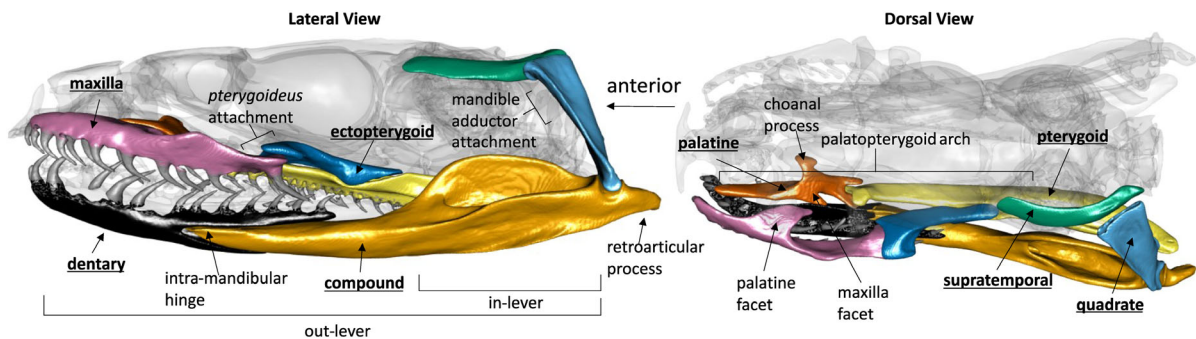
The kinetic skull is a key innovation that allowed snakes to capture, manipulate, and swallow prey exclusively using their heads using the coordinated movement of eight bones. Despite these unique feeding behaviors, patterns of evolutionary integration and modularity within the feeding bones of snakes in a phylogenetic framework have yet to be addressed. Here, we use a dataset of 60 μ CT-scanned skulls and high-density geometric morphometric methods to address the origin and patterns of variation and integration in the feeding bones of aquatic-foraging snakes. By comparing alternate superimposition protocols allowing us to analyze the entire kinetic feeding system simultaneously, we find that the feeding bones are highly integrated, driven predominantly by functional selective pressures. The most supported pattern of modularity contains four modules, each associated with distinct functional roles: the mandible, the palatopterygoid arch, the maxilla, and the suspensorium. Further, the morphological disparity of each bone is not linked to its magnitude of integration, indicating that integration within the feeding system does not strongly constrain morphological evolution, and that adequate biomechanical solutions to a wide range of feeding ecologies and behaviors are readily evolvable within the constraint due to integration in the snake feeding system.

KEY WORDS: Functional modularity, morphological evolution, morphometrics, Procrustes superimposition, skull, snakes.

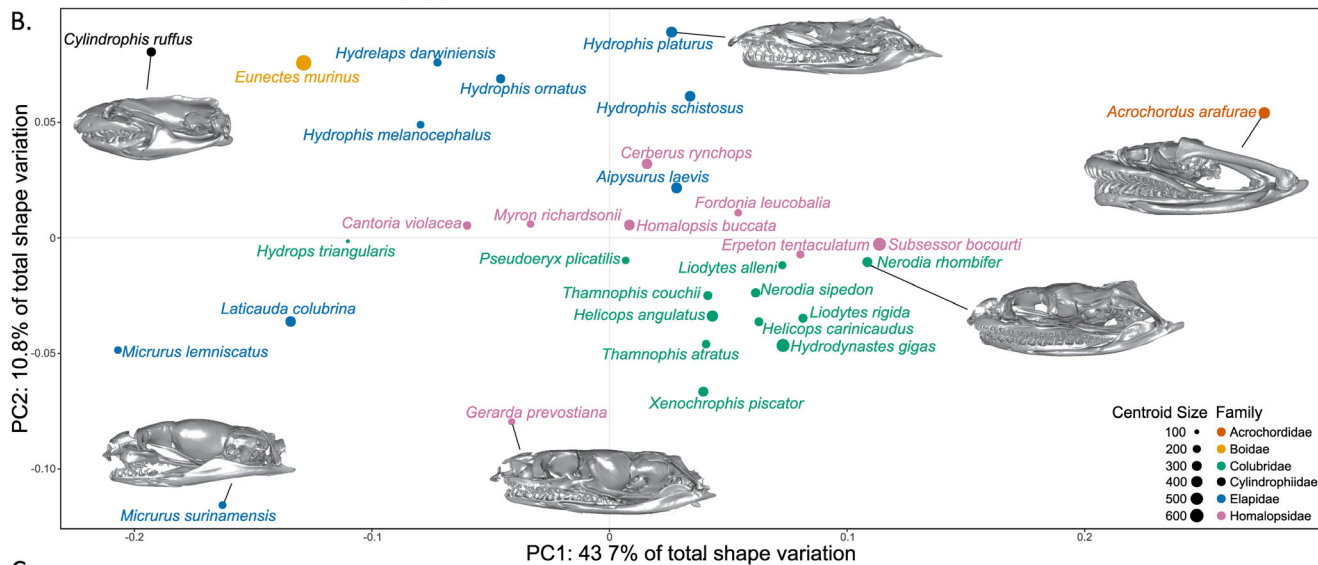
Morphological integration and modularity, defined as the covariances between anatomical traits (integration) and their partitioning into semi-autonomously varying modules (modularity), are key concepts in evolutionary biology and are present at some level in all organisms (Olson and Miller 1958; Wagner et al. 2007; Klingenberg 2008). Morphological integration may be advantageous for maintaining functional associations between traits; however, integration is expected to constrain morphological evolution when the direction of selection is not parallel to the line of least evolutionary resistance, defined by the phenotypic covariance matrix (Wagner and Altenberg 1996; Goswami et al. 2014; Melo et al. 2016; Felice et al. 2018). An integrated phenotype may therefore divert a lineage from evolving across an adaptive landscape along a direct path toward an adaptive peak, consequently deflecting evolutionary responses toward less fa-

voritable but more probable regions of morphospace. Modularity thus represents a compromise between complete independence between traits, which promotes evolvability but does not maintain functional associations, and complete integration, which constrains morphological evolution in nonviable ways (Wagner and Altenberg 1996; Goswami 2006). Accordingly, comprehension of the evolution of a clade across macroevolutionary timescales necessarily involves a detailed understanding of the clade's patterns of integration, as well as the processes that generate them. In this article, we examine patterns of morphological integration and modularity in the highly kinetic feeding system of aquatic-foraging snake skulls (Fig. 1). The acquisition of a higher degree of kinesis in the elements of the face and mandible compared to other vertebrates is a key evolutionary innovation (Caldwell 2019) that allowed snakes to radiate into over 3789 living species

A.



B.



C.

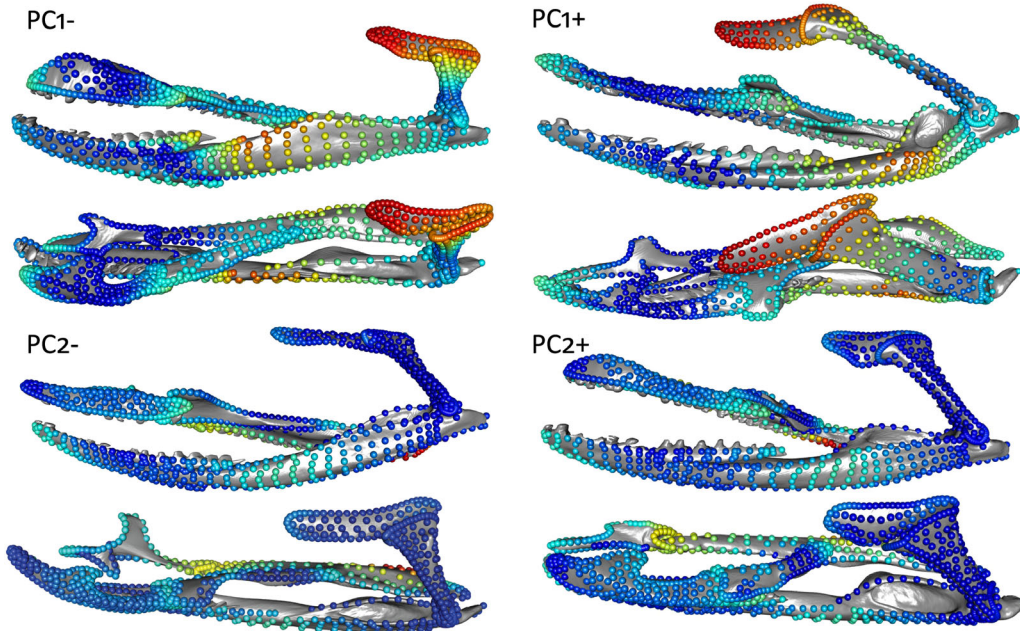


Figure 1. (A) The feeding system of snakes (colored) with the anatomical features referenced in this article labeled on a specimen of *Myron richardsonii* (AMNH R111792). The labels of bones studied here are underlined. (B) Scatterplot of the first principal components of a common superimposition of the whole feeding system. Each species is represented as an individual point, the size and color of which correspond to the centroid size (mm) and taxonomic family (see caption). (C) Shape variation along the first two principal components in lateral (top) and dorsal view (bottom), with landmark colors corresponding to the relative amount that each landmark varies along each PC axis (from PC- to PC+) with red (most variation) and blue (least variation).

(Uetz et al. 2019) encompassing a broad ecological, dietary, and geographic diversity.

The degree and organization of integration among anatomical traits is primarily caused by shared developmental origin and genetic linkages or functional relationships between traits (Olson and Miller 1958; Hallgrímsson et al. 2009). A morphological structure with multiple functions and developmental origins may be both functionally and developmentally modular, not necessarily in overlapping ways (Atchley and Hall 1991; Raff 1996). Disentangling the relative contributions of functional versus developmental modules will provide a fuller understanding of the macroevolutionary implications of morphological integration because their evolutionary lability reflects the lability and strength of the constraints that populations face in their evolution toward adaptive peaks. For example, if the pattern of evolutionary modularity is caused by a highly conserved suite of developmental pathways, then the macroevolutionary consequences of integration and modularity may be greater than if the same patterns were caused only by functional associations maintained by performance-based selection (Raff 1996). The feeding system of snakes (Fig. 1A) presents an opportunity to study how competing factors translate into patterns of morphological integration and modularity because it is both developmentally and functionally modular in patterns that do not match. If patterns of functional modularity match patterns of evolutionary modularity, then the functional relationships between traits are likely the primary driver of morphological integration.

Snakes are limbless tetrapods that forage almost exclusively using their heads (Cundall and Greene 2000; Moon et al. 2019). The hyperkinetic skulls of snakes are composed of over 20 bones articulated but unfused with one another, eight of which are directly involved in feeding (Fig. 1A). The extraordinary kinesis of the feeding system facilitates the independent movements of its individual bones, which allows exceedingly large gape sizes such that many snakes can ingest prey much larger than they are (Kardong 1977, 1979). The feeding bones are developmentally modular at least insofar that the different bones are ultimately the results of spatially separated developing cellular populations (i.e., the ossification centers of each bone do not meet to fuse together during development, but see Discussion; Raff 1996; Boughner et al. 2007; Polachowski and Werneburg 2013). Alternatively, the movements of these spatially separated bones must act in concert to successfully forage; snakes must capture, manipulate, and ingest prey exclusively using their head and anterior trunk (Cundall and Greene 2000; Moon et al. 2019). The feeding sequence of snakes can be divided into several segments: prey capture, prey manipulation and repositioning, and swallowing that includes the highly conserved “pterygoid walk” where the teeth of the palatine and pterygoid grasp and hold onto prey, whereas the braincase advances over it (Boltt and Ewer 1964; Cundall and Greene 2000;

Moon et al. 2019). The coordinated movement of different groups of bones is required to perform these different functions, forming functional modules. Bones within a functional module share selective pressures associated with their function and would be expected to covary over evolutionary time. Therefore, in the feeding system of snakes there exists a tension between the kinesis and developmental disintegration of bones promoting modularity and the functional dependencies between those bones promoting integration.

Snakes have independently invaded aquatic habits multiple times (over 360 species of snakes use aquatic media; Murphy 2012). The head shape of aquatic foraging snakes has functionally converged in response to the physical constraints related to prey capture under water (Fabre et al. 2016; Segall et al. 2016, 2019). Yet, aquatic-foraging snakes show a large amount of morphological variability along with an exceptional ecological diversity in terms of diet, behavior, and habitat use (Segall et al. 2020), which may be related to the disparate morphology of their feeding bones (Klaczková et al. 2016). The feeding sequence is highly constrained under water, from prey detection, to the hydrodynamic constraints generated by an accelerated strike (Segall 2019; Segall et al. 2020), to the subjugation and manipulation of slippery (e.g., fish, tadpoles), hard (e.g., crustaceans), and elongated preys (e.g., eels), to the lack of constriction in most species, to swallowing a (sometimes living) neutrally buoyant prey item (Moon et al. 2019). Piscivorous snakes present some specific morphological features in response to these functional constraints such as numerous, longer, sharper teeth (Savitzky 1983). Yet, the morphological and functional relationships between the different bones involved in the feeding sequence remain poorly studied.

In the present work, we use high-density three-dimensional (3D) geometric morphometrics on the eight bones that compose the feeding system of snakes to explore phylogenetically informed patterns of morphological integration and modularity within a large sample of species that share a functional constraint: aquatic foraging. We investigate morphological integration at all levels: within bones, between bones, and within the whole feeding system. To study morphological integration considering the whole feeding system, we compare two superimposition procedures allowing us to analyze separate mobile (articulating) bones at once, and then directly compare *a priori* hypotheses of modularity using the Covariance Ratio effect size (Adams and Collyer 2019). Focusing on a complex system involving the coordination of several morphologically disparate, developmentally disintegrated bones to fulfil a highly constrained behavior (aquatic foraging), this study aims to understand how functional and developmental modularity is translated into evolutionary integration and modularity, and how these patterns affect morphological disparity over macroevolutionary timescales.

Materials and Methods

SAMPLING AND SCANNING

Our taxonomic sampling consisted of 60 adult specimens representing 32 species of aquatic-foraging snakes from a wide taxonomic range (Fig. 1; Table S1). Specimens came from multiple Museum collections (AMNH, CAS, and FMNH) and were carefully chosen to have the mouth closed with no visible deformation or damage. We performed computed microtomography (CT) scans at a resolution between 15 and 50 μm , with the Phoenix v|tome| μ CT scanner (General Electric Company, Fairfield, CT, USA) at the AMNH Microscopy and Imaging Facility using a voltage between 100 and 150 kV and current between 130 and 160 mA for a voxel size between 15.6 and 57.4 μm . The 3D reconstruction of the whole skull was performed using the software Phoenix datos|x2 and the subsequent segmentation was done using VGStudioMax version 3.0 (Volume Graphics GmbH, Heidelberg, Germany). The dentary, compound (here defined as the portion of the mandible posterior to the intramandibular hinge, as in Andjelković et al. 2016, 2017), quadrate, supratemporal, pterygoid, ectopterygoid, palatine, and maxilla from the left side of each specimen were digitally separated from the whole skull in GeomagicStudio (3D Systems, Rock Hill). To facilitate the deployment of surface sliding semilandmarks, each bone was cleaned in Geomagic so that small holes were covered, teeth were removed, and surfaces were smoothed following the procedures suggested by Bardua et al. (2019a).

THREE-DIMENSIONAL GEOMETRIC MORPHOMETRICS

We used a high-density 3D geometric morphometric approach (1335 total landmarks across all bones) using both anatomical and semilandmarks, to quantify the shapes of each bone (Adams et al. 2004, 2013; Dumont et al. 2016; Goswami et al. 2019). Anatomical landmarks and curve semilandmarks were placed on each bone using IDAV Landmark Editor and MorphoDig (Fig. S1; Wiley et al. 2005; Lebrun and Orliac 2017). Using the function “placePatch” in the R package *Morpho*, surface landmarks were projected onto each separate bone from a template specimen following the precautions suggested by Schlager (2017) and Bardua et al. (2019a). Disparity in the shapes of the choanal and maxilla facet of the palatine obstructed the projection of surface landmarks, so the shape of the palatine was represented only with anatomical and curve landmarks. The choanal and maxilla processes were still captured with anatomical and curve landmarks. The curve and surface semilandmarks were allowed to slide to minimize bending energy (Gunz et al. 2005; Gunz and Mitteroecker 2013). We used generalized least-squares Procrustes superimposition with the “gpgen” function in *geomorph* (Rohlf and Slice 1990; Adams and Otárola-Castillo 2013) to analyze shape variation in each bone, individually.

SHAPE VARIABILITY, PHYLOGENETIC SIGNAL, AND ALLOMETRY

We used principal component analyses (PCA; “gm.prcomp” function in *geomorph*) to extract and visualize the main axes of variation for each bone and the whole feeding system (Adams and Otárola-Castillo 2013; see below for an account of how bones were combined to assess the feeding system as a whole). Thin-plate spline deformations applied on meshes were used to visualize the shape variation associated with each axis (“tps3d” function in *Morpho*). Using the phylogeny of Pyron and Burbrink (2014) pruned to our dataset (Table S1), we tested for a phylogenetic signal in each bone (“physignal” function in *geomorph*) to assess whether the phylogenetic relationships between species were related to their morphology (Adams and Otárola-Castillo 2013; Adams 2014). A significant phylogenetic signal was found in each bone ($P < 0.01$, $K < 0.59$; Table S2), so all subsequent analyses were performed in a phylogenetically informed context. To test for the effects of evolutionary allometry on shape, we performed phylogenetic generalized least squares analyses on the Procrustes coordinates and the log-transformed centroid size as a covariate using the “procD.pgls” function in *geomorph*.

MODULARITY ANALYSES AND SUPERIMPOSITION PROTOCOLS

As employed here, both eigenvalue dispersion and two-block partial least squares measure covariance in shape within and between bones independent of their relative sizes and positions in the mouth (discussed below). However, in the case of the feeding bones of snakes, the relative positions, orientations, and sizes of bones are immensely important to the functional relationships between bones and therefore morphological integration and modularity. For example, a larger gape in many taxa is accomplished by posterior rotation of the quadrate, such that the quadrate points posteriorly (see *Acrochordus arafureae*, Fig. 1B) rather than orthogonally to the mandible (as in *Cylindrophis ruffus*, Fig. 1B). Further, patterns of ontogenetic allometry in some macrostomatian snakes involve posterior rotation of the quadrate and positive allometry of the jaws, supratemporal length, and quadrate length (Scanferla 2016; Palci et al. 2016), facilitating ontogenetic niche shifts in some species (Mushinsky et al. 1982; Vincent et al. 2007). This allometric axis of shape variation, affecting separate component parts (i.e., potential modules) of the snake feeding system simultaneously, has been demonstrated to be functionally consequential, evolutionary labile, and adaptive (Esquerre et al. 2017 and Sherratt et al. 2019 report heterochronic shifts facilitating dietary shifts), suggesting that it may influence evolutionary integration within the snake skull. A shared coordinate system that maintains the relative sizes and positions of the bones is therefore desirable to understand the patterns of integration and modularity. We employed two superimposition strategies to

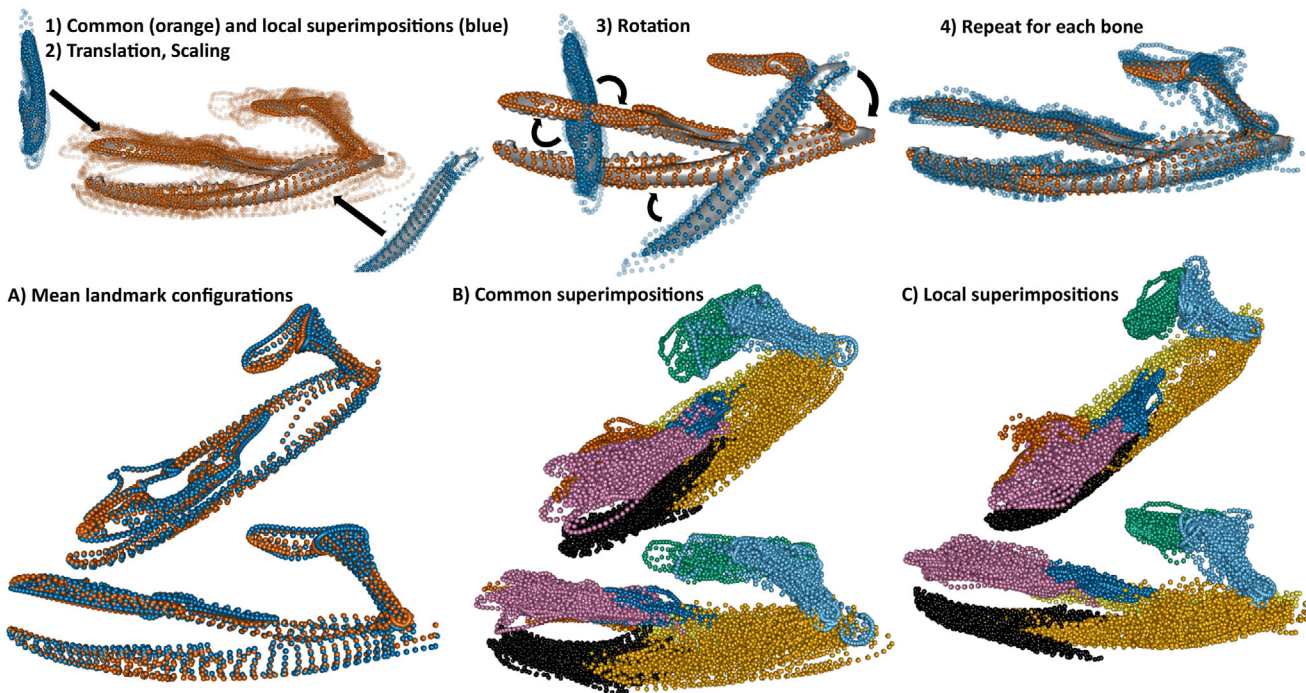


Figure 2. Workflow of the local superimposition procedure: (1) Procrustes superimpositions of the whole feeding system (i.e., common superimposition; GPA_{all}, orange) and of each individual bone (i.e., local superimpositions; blue) are performed. The transparent landmarks are individual species after their respective superimpositions. (2) Each local superimposition dataset is translated and scaled to the mean centroid size and position of its corresponding bone in the global mean shape from GPA_{all} and (3) rotated. (4) Final dataset for the local superimposed procedure. (Below) (A) Superimposition of the mean configurations of the common (orange) and local superimpositions dataset (blue). Complete landmark datasets for the common (B) and local (C) superimpositions procedures (color code matches Fig. 1).

achieve this goal: a common superimposition and “matched” local superimpositions.

The common superimposition consisted of performing a GPA on all of the bones at once in their original CT-scanned positions, treating them as if they were a single rigid structure (GPA_{all}) because in that position the bones all retain their relative sizes and are in a natural resting position relative to one another that is largely repeatable (it is worth noting that no “true” anatomical position exists in a kinetic system; Collyer et al. 2020). Mobility between the bones in a living snake is comparatively small relative to their overall position in this resting orientation (Watanabe et al. 2019; Fig. S2). Other authors have adopted a similar strategy for analyzing the shape of the entire feeding apparatus (e.g., Palci et al. 2016; Klaczko et al. 2016; dos Santos et al. 2017; Silva et al. 2018; Watanabe et al. 2019; Souto et al. 2019; Murtan Fonseca et al. 2019) and additional studies have superimposed nonrigid structures together in other organisms when taking appropriate precautions (Adams 1999, 2004; Rohlf and Corti 2000; Adams and Rohlf 2000; further discussed below). Each specimen was μ CT scanned with the mouths completely closed; only specimens in neutral poses were included, where articulating bones were positioned directly adjacent to each other. Even though none of the individual bones are fused with one another, numerous soft

tissue connections reduce rotational degrees of freedom of each bone. We also corrected for intraspecific variation by averaging landmark configurations per species, which further minimizes the variation due to mobility alone. The position and respective centroid size of each bone in the mean shape (of all species) resulting from this procedure were computed and used in the local superimposition procedure.

Because the relative positions of the elements could still vary nonrepeatably because of the death position in which the specimen was preserved, we also adopted a second approach: “matched” local superimpositions. This local superimposition procedure first consisted of performing a GPA for each bone separately. The superimposed landmark coordinates of each bone were then translated, rotated, and scaled to fit its corresponding bone of the mean shape from GPA_{all} (Fig. 2). This procedure allowed us to preserve the intrinsic, pure shape variation of each individual bone while placing landmarks of each bone within a common coordinate space. Further, the mean landmark configuration of the common superimposition, for which the local superimpositions were matched onto, was biologically realistic; because each specimen included was in a neutral pose, the landmark configurations average to a shape reflects a specimen in a neutral pose (Fig. 2), and specimens are scattered around the origin of the

PC morphospace suggesting that the mean configuration is natural and plausible (Fig. 1B). The interspecific positional and rotational variation between species may be large enough that it confounds interspecific patterns of pure shape variation within bones. The functional and developmental processes that govern the positional variation in bones may not be the same exact processes that govern pure shape variation within individual bones, and therefore support for alternative patterns of modularity may disproportionately reflect processes that control the positional variation in bones when only considering a common superimposition. The local superimposition procedure set landmark coordinate configurations in a coordinate space that was biologically realistic and reduced the positional and rotational variation due to mobility so that we could analyze patterns of modularity in the whole system while only considering pure shape (co)variation within the feeding system.

The two superimposition procedures are complementary: the local superimpositions account for pure shape variation in each bone and the common superimposition emphasizes (co)variation related to the overall configuration of the feeding apparatus. By comparing results from the two procedures, we bracket the “true” pattern of morphological, evolutionary modularity. If both superimposition procedures support similar hypotheses of modularity, then it is unlikely that the pattern arises because of arbitrary differences due to positioning of the mobile elements.

Removing the arbitrary differences in positioning of articulating structures is a longstanding issue in landmark-based morphometrics. Adams’ (1999) “Fixed Angle Method” and Vidal-Garcia and colleagues’ *shapeRotator* R package (Vidal-García et al. 2018) for 3D structures are approaches that minimize variation due to mobility by fixing the angle between articulating structures at their joint, for all specimens, and then performing a common superimposition as if the newly rotated articulating structure was rigid. These approaches have been used to answer a wide range of questions (e.g., Adams and Rohlf 2000; Adams 2004; Davis et al. 2016; Vidal-Garcia and Keogh 2017), and both rely on a set of arbitrary choices about how to position mobile elements relative to one another that do not have single fixed relative positions or orientations. Neither approach works well for snake cranial elements because they do not all articulate in positions consistent between species, nor do they operate as ordinary hinged joints. For example, *shapeRotator* positions articulated bones at the same angle with respect to each other and the joint, but the jaw joint of a snake effectively has two joints, one at the distal end of the quadrate and another at the proximal end. The resting angle of these joints differs from species to species depending on the relative length of the quadrate. For example, if we fixed the angle of the quadrate across all specimens so that its long axis was perpendicular to the mandible, as in *Cylindrophis ruffus* (Fig. 1B), it would displace the cranial el-

ements dorsally in *Acrochordus arafurae* because the quadrate is proportionally longer in *Acrochordus*. Thus, there is no single angle of the quadrate that brings the mandible and upper jaw into their natural closed position across all snakes because it is not a simple hinge. For this reason, we developed the “local superimpositions” strategy described above that positions the bones at the angles and locations of the animal when its mouth is closed and relaxed rather than previous published strategies that were optimized for different anatomical systems. To show how results are affected by these choices, the Supporting Information presents reanalyses using two variations of *shapeRotator*’s strategy (Text S1). Although those results differ in detail, the overall outcomes are the same.

MORPHOLOGICAL INTEGRATION AND MODULARITY ANALYSES

We used three methods to analyze the pattern of morphological integration and modularity. Relative eigenvalue standard deviation (eigenvalue dispersion) was employed to measure the overall degree of morphological integration within each bone and then the feeding system as a whole (Pavlicev et al. 2009). Phylogenetic two-block partial least squares (2BPLS, “phylo.integration” function in *geomorph*) analyses were used to assess morphological integration between each pair of bones (Rohlf and Corti 2000; Adams and Felice 2014; Adams and Collyer 2016). The Covariance Ratio was used to test a priori hypotheses of modularity based on the whole feeding system (Adams 2016; Adams and Collyer 2019).

Eigenvalue dispersion was calculated from a singular value decomposition of the covariance matrix of the Procrustes-superimposed landmark configurations for each bone. Higher eigenvalue dispersion values correspond to larger degrees of morphological integration because a smaller number of eigenvectors will explain a larger portion of total correlated shape variation in more-integrated structures (Goswami and Polly 2010a; Pavlicev et al. 2009). Eigenvalue dispersion values range between 0 and 1 and are comparable across datasets (e.g., different bones; Pavlicev et al. 2009).

The degree and significance of morphological integration between each pair of bones was quantified using phylogenetic 2BPLS and its effect size (Rohlf and Corti 2000; Adams and Felice 2014; Adams and Collyer 2016). For each pair of significantly integrated pairs of bones (P -value < 0.05), we describe shape variation along the primary axis of covariation (PLS1) to determine which anatomical structures contribute to covariation (Fig. 3). To test if the magnitude of integration constrains morphological diversity, we conducted two least-squares linear regression analyses with Procrustes variance values (i.e., morphological disparity) against (1) eigenvalue dispersion values (i.e.,

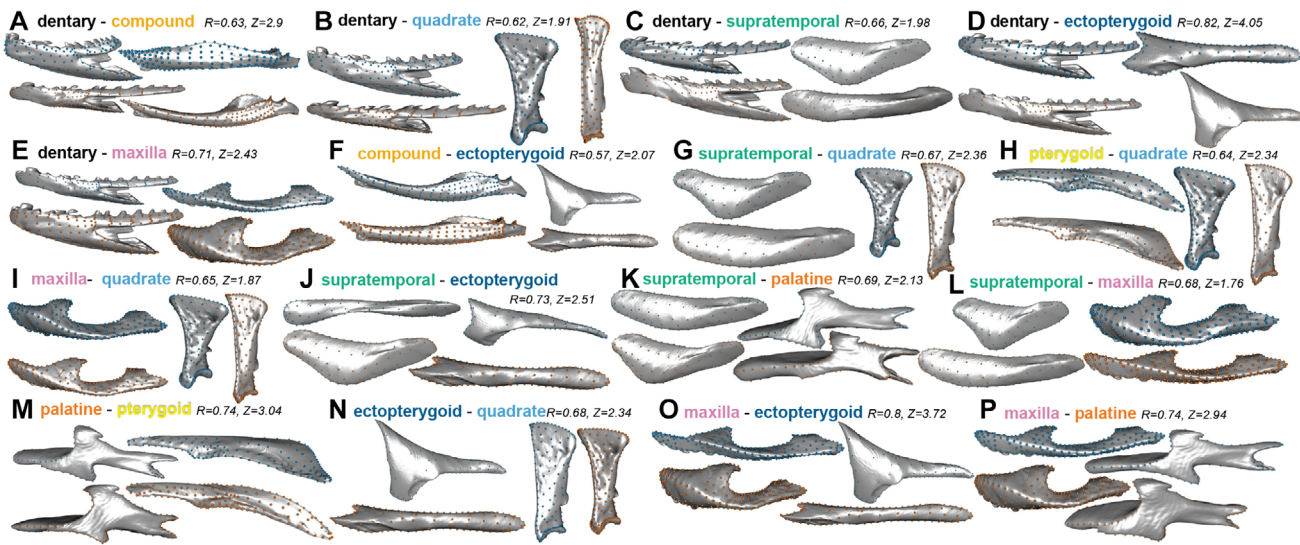


Figure 3. Pairwise shape covariation in snake feeding bones along PLS1 from each significant phylogenetic 2BPLS. Blue: PLS1-; Orange: PLS1+. Z and R scores are indicated.

within-bone integration) and (2) the average 2BPLS effect size for each bone (i.e., between-bone integration) (Fig. 4).

For both superimposition methods, 21 a priori hypotheses of modularity were tested using the CR (Adams 2016; Adams and Collyer 2019). Each hypothesis of modularity was based on combinations of associations of bones that would be expected to covary in certain functional or developmental contexts (Table S3).

To visualize the major axes of correlated shape variation within each module of the most supported hypothesis, we performed phylogenetic PCAs (pPCA; Revell 2009; Adams and Collyer 2018) on each module (“gm.prcomp” in *geomorph* with the “Transform” and “GLS” parameters set to “True”). Bones within each module were superimposed together. These per-module superimpositions were not used for any statistical analysis and were only used for visualization purposes. Shape variation along pPC1 was visualized because it is the axis of most correlated shape variation within each module while accounting for phylogenetic non-independence.

Results

SHAPE VARIATION AND COVARIATION OF INDIVIDUAL BONES

Significant allometries were found in the quadrate, supratemporal, palatine, and maxilla but explained only a small portion of the shape variation ($R^2 = 0.6\text{--}0.8$) except for the quadrate ($R^2 = 0.26$; Table S2). There was no significant allometry in the dentary, compound, pterygoid, and ectopterygoid. The largest eigenvalue dispersions (i.e., within-bone integration) were reported in the compound (0.648) and ectopterygoid (0.645) and the smallest in the

supratemporal (0.451) and maxilla (0.465) (Table S2; Fig. 4) (see Figs. S3-S10 for individual bone variation description). Linear regression analysis showed that the degree of morphological integration within each bone did not significantly relate to morphological disparity (P -value = 0.44; Fig. 4). Our 2BPLS analyses recovered significant integration between 16 out of 28 possible pairs of bones (Tables S4 and S5; Fig. 3). The pterygoid is only significantly integrated with the quadrate and palatine, and the compound is only significantly integrated with the dentary and ectopterygoid. The palatine is also integrated with fewer bones (3) than any of the other bones (each is integrated with five other bones) (Fig. 3; Tables S4 and S5). The most strongly integrated pairs are ectopterygoid/dentary (r -PLS = 0.822; Fig. 3D) and the ectopterygoid/maxilla (r -PLS = 0.806; Fig. 3O). Descriptions of shape variation along PLS1 are provided in the Discussion and shown in Figure 4. The average 2BPLS effect size for each bone did not significantly relate to morphological disparity (linear regression analysis, P -value = 0.173; Fig. 4B).

SHAPE VARIATION OF THE WHOLE FEEDING APPARATUS

Significant allometry was recovered for both the common and local superimposition datasets containing all bones (P -value = 0.001, $R^2 = 0.13$ and P -value = 0.018, $R^2 = 0.07$, respectively). The common superimposition showed a larger eigenvalue dispersion value (0.447) than the local superimposition dataset (0.352).

The first principal component (PC1) of the common superimposition dataset (Figs. 1B and 1C) accounts for 43.7% of the overall shape variation in the feeding apparatus of snakes and is mainly driven by the orientation and length of the quadrate, as well as slenderness of the mandible and maxilla, and mechanical

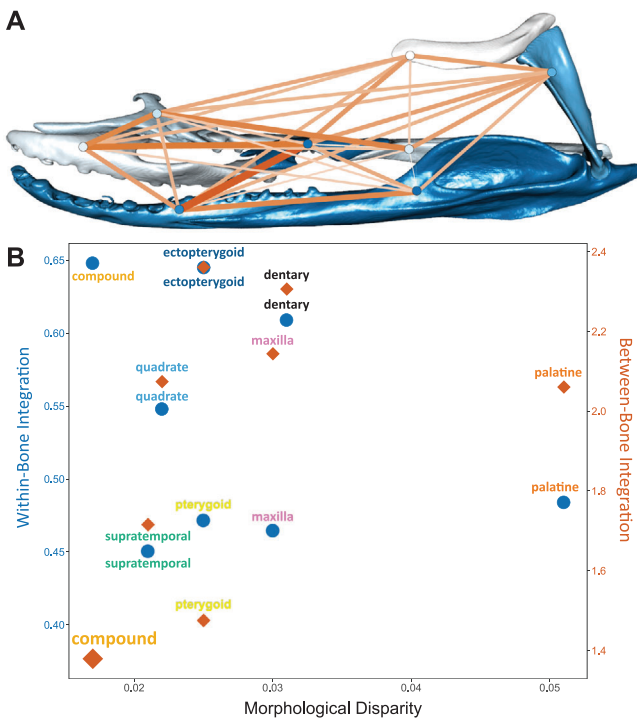


Figure 4. (A) Network graph of within- and between-bone integration in the feeding apparatus. Within-bone integration (eigenvalue dispersion values) is represented by the bone color: the darker, the stronger. Covariation between bones (2BPLS effect size; z-PLS) is represented by the color and width of the line connecting each pair of bones: wider and darker connections correspond to higher effect sizes and stronger morphological integration between the bones (values in Tables S2, S4, and S5). (B) Scatter plots of morphological disparity (x-axis) with within-bone integration (eigenvalue dispersion, blue points, left y-axis) and between-bone integration (average all the z-PLS for each bone, orange points, right y-axis). Both regression analyses were not significant.

advantage of the mandible. Shapes at the positive extreme of PC1 (PC1+) had a longer and posteriorly rotated quadrate, and elongated, slender mandibles and maxillas. A ventrally bowed mandible and prominent palatine processes were characteristic of shapes at PC2-. Colubridae grouped together except *Hydrops triangularis* (Colubridae) that was separated along PC1, and Homalopsidae are grouped along PC2, except the crab-tearing specialist *Gerarda prevostiana* (Homalopsidae; Jayne et al. 2002; Jayne et al. 2018). The elapids showed substantial variation along both PC axes and drive the variation of PC2, with the true sea snakes (Hydrophiinae) grouping at PC2+ and the semi-aquatic coral snakes (Micrurinae) at PC2-. *Acrochordus arafureae*'s exceptionally elongated mandible and quadrate drive the variation along PC1+, whereas species on PC1- have a short and almost horizontally positioned quadrate and a dorsally expanded prearticular process. Shape variation along PC2 is smaller (10.8% of total variation), and mainly carried by variation in the palatine-

pterygoid joint. Species at PC2- have a dorsolateral expansion of the posterior part of the pterygoid and a simple shape of the palate-pterygoid articulation, whereas species at PC2+ have a slender pterygoid with a complex articulation shape.

MODULARITY IN THE WHOLE FEEDING APPARATUS

The most supported hypothesis (i.e., the most negative Z_{CR} value, meaning the strongest modular signal) for both common and local superimpositions datasets described two modules (Fig. 5; Table S6A). The most supported hypothesis from the common superimposition (H1) described dorsoventral modularity with mandibular (dentary, compound) and nonmandibular elements as separate evolutionary modules. The most supported hypothesis from the local superimposition dataset (H4) was also composed of two modules, one with the dentary, compound, maxilla, and quadrate and the other with the supratemporal, ectopterygoid, pterygoid, and palatine, describing a lateromedial pattern of modularity. Hypothesis 15 (H15; Fig. 6; Tables S3 and S6) was the third and second most supported hypothesis in the common and local superimposition dataset, respectively (Fig. 5). H15 described four modules: the mandible; a module with the pterygoid, palatine, and ectopterygoid; the quadrate and supratemporal as a module; and the maxilla as an independent module. Complex hypotheses of modularity (i.e., complete modularity, H21) were not as strongly supported as hypotheses with four or less modules (Table S6). PCA morphospaces and Z_{CR} results from the two new fixed-angle datasets are largely congruent with results from our common and local superimposition datasets (Table S6; Fig. S11).

DISCUSSION

In the present work, we quantified and compared morphological variability of eight bones that work jointly to fulfill a fitness-relevant function (i.e., feeding), at different levels of organization, from covariation within individual bones to patterns of integration and modularity considering all bones, in a phylogenetically informed context. Our results suggest that the feeding apparatus of snakes is highly integrated, predominantly driven by functional relationships between the bones. Our most supported hypotheses describe the mandible and the palatopterygoid arch (i.e., palatine and pterygoid) as two separate modules, with the maxilla and quadrate either integrated with the cranial elements (common superimposition) or the mandibular elements (local superimpositions). The hypothesis with the strongest support from both datasets, H15, contains an integrated palatopterygoid arch (including the ectopterygoid), the maxilla as an independent module, the quadrate and supratemporal as a module, and the mandible as a module. This considerable degree of integration is interesting considering the extreme kinesis of the feeding system, a factor we would generally expect to promote modularity

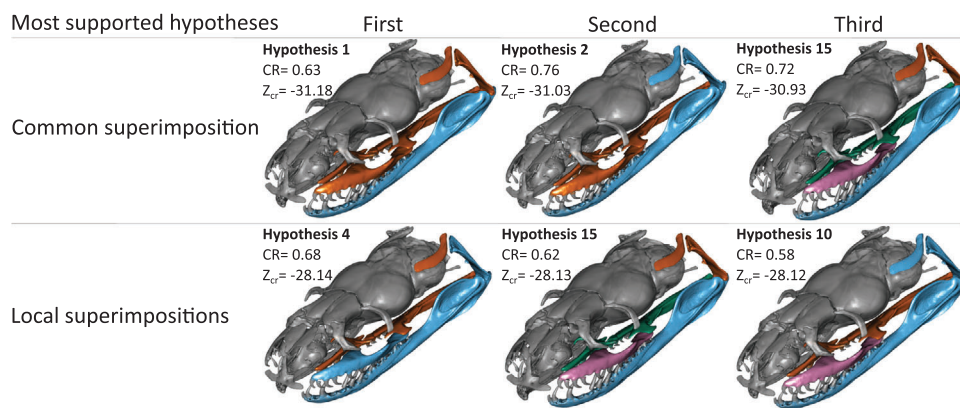


Figure 5. The three most supported hypotheses of snake feeding bone modularity for each superimposition method. Each group of similarly colored bones describes a module. The lower the effect size (Z_{CR}), the stronger the modular signal, and the more supported the alternative hypothesis. The order of most support is supported by pairwise effect size P-values (Figure S12). Note that hypothesis #15 (with four modules) is the only hypothesis supported strongly by both superimposition methods.

because the bones are not physically coupled with one another and have the freedom to move (and evolve) independently. The high degree of integration within the feeding system supports functional relationships between bones as the primary driver of integration, as the synchronized movements of different combinations of feeding bones are necessary for successful foraging (further discussed below; Cundall and Greene 2000; Moon et al. 2019). These findings also corroborate a recent study by Watanabe et al. (2019) who found that the crania of snakes are highly modular, except for the palatopterygoid arch. Although only four bones overlap between their study and ours (the distal quadrate “jaw joint,” maxilla, pterygoid, and palatine), we report generally consistent patterns of modularity in the most supported hypotheses (Figs. 5 and 6), with an integrated palatopterygoid arch separated from the maxilla and quadrate. Although the maxilla and quadrate are a part of the same module in our most supported hypotheses, they show a moderately low degree of integration, and are a part of separate modules in many other highly supported hypotheses, as is discussed below. Moreover, Watanabe et al. (2019) speculated that cranial kinesis may promote integration; we find exceptionally strong integration when considering the most mobile elements of the hyperkinetic snake skull.

FUNCTIONAL AND MORPHOLOGICAL INTEGRATION IN THE FEEDING SYSTEM

Our most supported hypotheses of modularity are consistent with a pattern that arises from functional aspects of feeding. Prey ingestion is accomplished in most advanced snakes via the “pterygoid walk,” involving the coordinated movement of the palatine and pterygoid bones (palatopterygoid arch) (Boltt and Ewer 1964; Cundall 1983); accordingly, there are shared functional selective pressures between these bones. During the pterygoid

walk, the palatopterygoid arch teeth grasp prey, whereas the braincase advances over it. This function is crucial for foraging in snakes and its performance is especially fitness related in macrostomatian taxa that ingest large prey, as snakes are vulnerable to predators during the pterygoid walk (Cundall and Greene 2000). In aquatic-foraging snakes, selective pressures associated with swallowing may be exacerbated due to the lubriciousness of prey, or the fact that there may not be a substrate to anchor onto during the pterygoid walk. The palatine and pterygoid were integrated in our 11 most supported hypotheses from the common superimposition, and eight most supported from the local superimposition dataset. In fact, the hypothesis of complete modularity besides the palatopterygoid arch (H19) was much more supported in both datasets than the hypothesis of complete integration besides the palatopterygoid arch, indicating that the palatopterygoid arch contributes substantially to covariance patterns when considering the whole feeding apparatus. According to 2BPLS analyses, neither the palatine nor pterygoid are integrated with more than three different bones. Andjelković et al. (2017), who also found low integration between the pterygoid and other bones, hypothesized that the pterygoid’s functional optimization prevents it from covarying with other bones. Considering the pterygoid’s integral role in prey ingestion (hence the “pterygoid walk”) and its physical entanglement with multiple other bones either through articulations or muscle attachments, functional optimization may explain the pterygoid’s high integration when considering the whole feeding system but not in 2BPLS analyses. The pterygoid and palatine are also the first bones in the feeding system to ossify (Sheverdyukova 2019; Polachowski and Werneburg 2013; Khannoon and Evans 2015; Werneburg et al. 2015), which may promote integration between them (and disintegration between the palatopterygoid arch and the rest of the system) either because

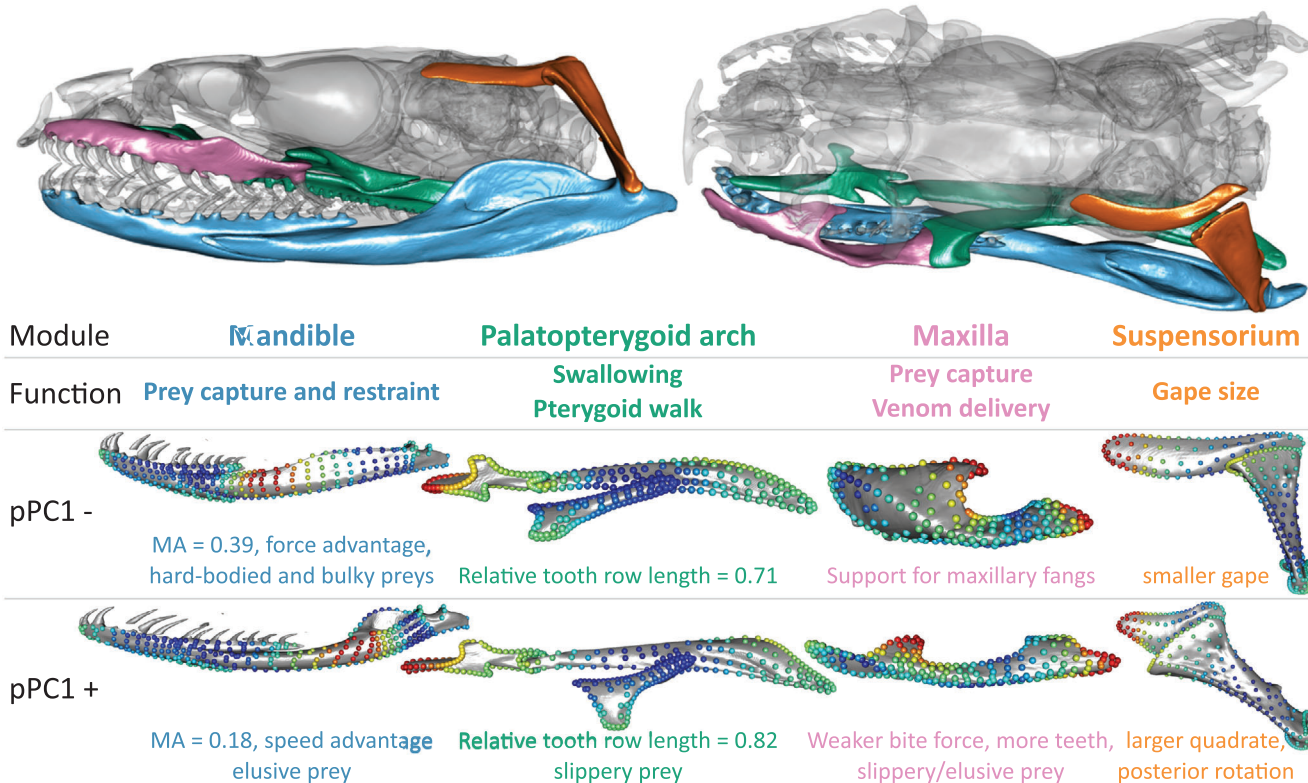


Figure 6. A four-module hypothesis (H15) where each module is associated with a distinct functional selective pressure is strongly supported by both superimposition procedures. (Above) Snake skull with the different modules highlighted in different colors in lateral (left) and dorsal (right) view. (Bottom) Per-module shape variation and their functional consequences along phylogenetic PC1. Relative tooth row length was calculated as (length of palatine tooth row + length of pterygoid tooth row) / total anterior-posterior length of the palatopterygoid arch. The color of landmarks represents the magnitude of its variation along pPC1 with red dots varying the most.

of additional, shared opportunity for bone remodeling during development or a shared influence of morphogens expressed during the palatopterygoid arch's early ossification that the other bones do not face.

Strong functional selective pressures drive integration within the mandible as well. The mandible, particularly the compound bone, is directly involved in multiple functional modules. The jaw adductor, responsible for closing the lower jaw and necessary for prey capture, originates on the anteroproximal quadrate and inserts on the mandibular fossa of the compound (Johnston 2014). The *pterygoideus*, which moves the palatopterygoid arch ventromedially and the dentary row dorsolaterally during prey ingestion, attaches on the retroarticular compound process and either the ectopterygoid or maxilla (Cundall 1983; Jackson 2003; Johnston 2014; Fig. 1A). Therefore, we would expect the compound to be integrated with the dentary, quadrate, ectopterygoid, and maxilla if functionally relevant muscles solely cause morphological integration. Yet 2BPLS results reveal there is significant integration only with the dentary and ectopterygoid. The PC morphospace and 2BPLS results both suggest that selection for mechanical advantage (MA) is the primary driver of inte-

gration within the mandible. The main component of variation in the compound bone (PC1), that accounts for almost 65% of the variation, describes the ratio of the in-lever to the out-lever (Fig. 1A). PC1 of the dentary describes variation in its slenderness and relative length (Fig. S4). Shape variation along PLS1 of the dentary and compound mirrors this shape variation (Fig. 3A). Taken together, the main axes of variation (PC1) and covariation (PLS1) in the dentary and compound cumulatively describe variation in the MA of the species. Species with a low MA (a longer out-lever compared to in-lever) have a speed advantage and are adapted for capturing elusive prey, and species with a high MA will have a force advantage and are adapted for capturing hard-bodied or bulkier prey (Wainwright and Richard 1995; Mori and Vincent 2008; Hampton 2011). Selection for MA almost certainly promotes integration between the dentary and compound because both separate bones contribute to MA. Further, jaw MA has been related to dietary niche (Mori and Vincent 2008; Hampton 2011), meaning that selection for dietary specializations may promote integration within the mandible. The dentary and compound were significantly integrated (2BPLS, Tables 4 and 5) and were a part of the same module in our four most supported

hypotheses of modularity (Table S6). This substantial integration within the mandible is functionally relevant, and is particularly interesting considering the evolution of the intramandibular hinge that can be considered a form of developmental disintegration in that ossification centers of the dentary and compound do not fuse, a process we would expect to promote modularity, especially if inhibitory signaling obstructs fusion of the ossification centers (Raff 1996). The anatomical liberation between component parts of the mandible is functionally adaptive, as it allows greater mobility and a larger gape (Kardong 1977); in the mandible, we find strong morphological integration directly from developmental disintegration.

DIETARY NICHE AND MODULARITY

If the relative importance of different functional modules relates to dietary niche, then it is reasonable to assume that patterns of modularity are influenced by the selective pressures associated with both prey properties and feeding behaviors. For example, eels require different manipulation skills than crabs; however, capturing and restraining hard-bodied crabs may require a stronger bite force than required to capture an eel. Consequently, an eel specialist may exhibit a covariance structure such that features associated with prey manipulation are more strongly integrated than features unique to prey capture, and vice versa in a crab-specialist taxon.

The *retractor pterygoideus*, which originates on the braincase and inserts on the medial palatine along the choanal process, is responsible for advancing the braincase over the prey during the pterygoid walk. The shape of the choanal process on the palatine (C8 and C9; Fig. S1) is highly variable along PC2 of the common superimposition, and both PC axes of the palatine morphospace (Fig. S9). The venomous, pelagic *Hydrophis platurus* completely lacks a choanal process but contains an elongated retroarticular process, providing substantial area for attachment of the *pterygoideus* muscle. Stimulation of the *pterygoideus* muscle induces outward rotation of the dentary tooth row (Cundall 1983). The primary role of the mandible in many taxa during ingestion is to keep prey pressed onto the teeth of the palatopterygoid arch. In a venomous, pelagic sea snake adapted for elusive and neutrally buoyant prey, selective pressures for prey ingestion may be stronger on morphological features relevant to prey manipulation and handling rather than advancement of the braincase over bulky, less mobile prey, consequently creating different patterns of integration involving areas of attachment for these or other cephalic muscles. The degree to which prey properties, particularly shape or bulkiness, affect patterns of integration in the feeding system of snakes by reorganizing the relative importance of different, overlapping, functional modules should be investigated in further detail. Additionally, the alternative modes of prey ingestion adapted to a broad range of prey types

(e.g., mandibular raking, Deufel and Cundall 2003, or sawing, Kojima et al. 2020, or tearing prey, Jayne et al. 2018) illustrates the interspecific variation in myological and functional relationships between the feeding bones. Future studies should examine intraspecific modularity in a select number of taxa at phylogenetically and ecologically informative positions to control for this variation in functional modularity, and to further incorporate within-bone modularity into hypotheses of modularity of the whole feeding system. Accompanying these morphometric analyses with empirical measurements of functional performance (e.g., manipulation and swallowing durations) will provide a better understanding of the factors shaping patterns of integration and modularity in the feeding bones of snakes, specifically how shifting functional relationships between anatomical regions translate into phenotypic covariance.

MORPHOLOGICAL INTEGRATION IN THE MAXILLA AND UPPER JAW

The placement of the maxilla in either the palatopterygoid arch module, the suspensorium module, or as an independent module is not apparently clear. Cundall (1983) argued for a medial swallowing functional module, composed of the palatopterygoid arch, and a lateral prey capture functional module, composed of the maxilla and ectopterygoid, in the upper jaw. This functional modularity hypothesis is supported in the local superimposition but not common superimposition results, as the two functional modules are integrated together in the two most supported hypotheses of the common superimposition. The functional dissociation between the lateral and medial upper jaw was noted by Cundall (1983) because the maxilla plays a minimal direct role in ingestion. Yet, the morphological integration between the two suggested functional modules does not prevent the bones to be involved in different functions. Moreover, the maxilla articulates with the palatine and the ectopterygoid, which articulates with the pterygoid, and the presence of maxillary fangs dramatically restructures the morphology of the maxilla such that some “advanced” (alethinophidian) snakes ingest prey using different mechanisms such as mandibular adduction because of the biomechanical limitations from modified cranial morphology due to the presence of maxillary fangs (Deufel and Cundall 2003). A modification in the morphology of the maxilla may then necessarily correspond with modifications in the other elements of the upper jaw because of these articulations, promoting integration within the upper jaw. This is especially true when considering positional information as in the common superimposition but is also captured in PLS1 of the maxilla-palatine integration, which shows that shape covariation between the two bones is dominated by their common joint surfaces (Fig. 3). So, although the upper jaw may behave as an evolutionary module, the maxilla and ectopterygoid’s incorporation into this module may be because

of structural and physical associations with the palatopterygoid arch, rather than purely functional relationships. This is an important point because morphological integration caused by structural associations between bones is certainly present in the feeding system of snakes; however, particularly structurally integrated, fused structures such as the avian cranium show highly complex patterns of modularity (seven modules; Felice and Goswami 2018) despite morphological evolution in one bone necessarily involving the evolution of neighboring bones because they must fit together. Yet, in the hyperkinetic snake feeding apparatus, the most supported hypotheses of modularity describe two to four modules out of eight completely unfused bones.

MODULARITY AND SUPERIMPOSITION PROCEDURES

Comparing shape (co)variation of a common superimposition and local superimpositions enabled us to analyze separate mobile elements simultaneously and compare the strengths and weaknesses of each method for analyzing modularity. The presence of the maxilla in different modules depending on which superimposition method is used demonstrates the influence that incorporating positional information (GPA_{all}) or isolating pure shape variation (local superimpositions) has when examining patterns of morphological modularity. The maxilla's integration with the suspensorium when only considering pure shape variation (local superimpositions) is corroborated in PLS1 shape variation of the dentary, quadrate, maxilla, and ectopterygoid, which all showed consistent patterns of shape covariation with one another such that a robust dentary and maxilla, a quadrate with a wider proximal end, and a slender ectopterygoid lied at similar ends of PLS1, as did the combination of a slender dentary and maxilla, a slender and longer quadrate, and a wider anterior ectopterygoid (Fig. 3). This collection of bones that covary along consistent axes of shape covariation with each other may reflect a functional trade-off between snakes adapted for elusive versus hard-bodied prey; a robust dentary and maxilla is better suited for prey capture than manipulation or ingestion, and a wider proximal quadrate provides additional area for attachment of the mandibular adductor muscle that may increase bite force (Fig. 1A). Comparing superimposition methods revealed competing factors contributing to the maxilla's integration within the feeding system: local superimpositions revealed shared functional selective pressures integrating the maxilla with the suspensorium, and the common superimposition revealed structural associations integrating the maxilla with the palatopterygoid arch. The fact that the common superimposition dataset showed a higher magnitude of overall morphological integration than the local superimposition dataset suggests that incorporating positional information contributed to the magnitude of integration (Table S2). Allometry also had a greater effect on the common superimposition dataset, possibly

due to posterior rotation of the quadrate dominating variation in landmark coordinates.

Although the different superimposition methods do not support the same first hypothesis of modularity, both methods strongly support Hypothesis 15 (Figs. 5 and 6), describing four modules with relatively distinct functional roles. In this hypothesis of modularity, the palatopterygoidarch including the ectopterygoid forms a module, driven by the highly conserved translational movement of the palatopterygoid arch during the pterygoid walk. The maxilla evolves as an individual module, possibly due to the competing structural versus functional influences explained above. The mandible is another module, highly integrated via selection for mechanical advantage. The quadrate and supratemporal, which articulate the feeding apparatus with the braincase, form the last module in this hypothesis, most likely coupled by a shared selective pressure for gape size. Although the mandible also contributes to gape size, it is highly constrained by mechanical advantage as discussed above, and the posterior rotation of the quadrate dominates PC1 of the common superimposition (describing nearly half of the total shape variation; Fig. 1B), which is plausibly how, more specifically, a larger gape size is accomplished, thus making the quadrate and supratemporal its own evolutionary module. Further, the largest degree of evolutionary allometry was found in the quadrate; Palci et al. (2020) did not find significant evolutionary allometry in the quadrate when considering all Squamata, so the allometry found here likely relates to gape size and is adaptive.

Because different integration inducing functional, developmental, and genetic processes may affect shape, positional, and size variation unevenly, our use of common and local superimpositions attempts to bracket the “true” pattern of modularity. Moreover, eigenvalue dispersion and 2BPLS results, which are independent of rotational and positional variation, were largely consistent with CR results. H15 is possibly the pattern in which component parts of the feeding system evolve semi-independently, as both superimposition methods strongly support it; however, there may exist an even less complex pattern of modularity considering that two-module hypotheses were most supported in both methods.

DOES THE MAGNITUDE OF MORPHOLOGICAL INTEGRATION CONSTRAIN MORPHOLOGICAL DIVERSITY?

Previous work has shown that the strength of integration can facilitate (Randau and Goswami 2017a; Navalón et al. 2020; Fabre et al. 2020), constrain (Goswami and Polly 2010b; Felice et al. 2018), or have no recoverable effect on morphological diversity (pedomorphic salamanders in Bardua et al. 2019b, 2020; Watanabe et al. 2019; Fabre et al. 2020; Bon et al. 2020). Here, we find that neither the strength of within-bone integration nor the

average strength of each bone's association with another has a significant effect on morphological diversity (Fig. 4B). As such, the considerably high degree of integration within the feeding system of aquatic-foraging snakes does not seem to affect morphological diversity over macroevolutionary timescales. This finding is interesting when considering the ecological and functional diversity of aquatic-foraging snakes, as it indicates that sufficient mechanical solutions to a broad range of feeding behaviors and diets are readily accessible within the highly integrated hyperkinetic feeding system of aquatic-foraging snakes.

THE HYPERKINETIC FEEDING SYSTEM IS HIGHLY INTEGRATED

Despite the kinesis in the feeding system of snakes, the individual bones are highly integrated with one another and organize into two to four evolutionary modules (Figs. 5 and 6). In fact, the extreme kinesis is the reason why the feeding systems of snakes is so functionally optimized and thus so highly integrated (Cundall and Greene 2000; Moon et al. 2019). The developmental disintegration necessary to anatomically liberate fused structures implies that snake feeding bones oppose an expectation in morphological integration and modularity literature that suggests that functional systems may adaptively evolve in congruence with developmental systems or vice versa (Cheverud 1984, 1996; Wagner and Altenberg 1996; Klingenberg 2014). Of course, this does not consider alternative modes of developmental integration between separate bones, such as shared gene expressions, pleiotropic effects, or shared embryonic origin. Developmental systems can integrate spatially separated features as well, such as serially homologous limb bones (Hallgrímsson et al. 2002; Bell et al. 2011) or vertebrae (Randau and Goswami 2017a,b, 2018; Jones et al. 2018, 2020; Arlegi et al. 2020). Accordingly, it is possible that the evolutionary and functional modules of H15 (Figs. 5 and 6) also match some pattern of developmental or genetic modularity. In any case, our developmental modularity hypotheses, which considered the embryonic origins of the articular and quadrate (splanchnocranum) and the rest of the feeding bones (dermatocranum), were not well supported (Table S5). Although additional patterns of developmental integration potentially contributing to morphological integration in the snake skull are less understood but surely exist, the high amount of morphological integration in the kinetic feeding system of snakes is striking when considering the complex patterns of modularity recovered from the synostotic bones that make up akinetic morphological structures in mammals (Goswami 2006; Martín-Serra et al. 2020; Adams and Collyer 2019), archosaurs (Felice and Goswami 2018; Felice et al. 2019), and amphibians (Bardua et al. 2019b; Bardua et al. 2020; Marshall et al. 2019; Bon et al. 2020; Fabre et al. 2020). In the feeding system of aquatic-foraging snakes, we

recognize strong functional and evolutionary integration generated because of its kinesis and developmental disintegration.

Conclusion

In this article, we quantify shape variation in the hyperkinetic feeding system of a phylogenetically broad sample of aquatic-foraging snakes and review patterns of morphological integration and modularity within this system. We find that the feeding system is highly integrated, with the most supported hypotheses of modularity involving only two modules despite there being eight separate bones unfused with one another. The most supported patterns of modularity describe an integrated palatopterygoid arch and mandible as separate modules, with the maxilla and quadrate either part of the palatopterygoid arch or mandible module depending on whether positional information was preserved in the superimposition method. Regardless, both superimposition methods show strong support for a four-module hypothesis with each separate module responsible for a specific functional role. This four-module hypothesis may be the best representation of how different regions of the feeding system independently evolve. Indeed, the major axes of phylogenetically informed shape variation of each of these modules have considerable functional consequences (Fig. 6), suggesting that modularity and integration is primarily influenced by performance-based selective pressures associated with feeding ecology. The utility of comparing common and local superimpositions of a mobile system to “bracket” the most biologically accurate pattern of modularity proved fruitful and may be considered in future studies when taking appropriate precautions. Further, the relatively high degree of integration in this hyperkinetic system is fascinating when considering the developmental disintegration necessary to spatially disintegrate each component part, and the complex patterns of modularity found in fused structures such as rodent mandibles (Adams and Collyer 2019). Despite this exceptionally strong integration within the feeding system, morphological diversity is not apparently constrained, indicating that adequate mechanical and functional solutions to a wide variety of dietary and ecological niches are readily available within constraint due to integration in the feeding system. Further research addressing morphological integration in the skull of snakes with different dietary challenges (e.g., arboreal species, snail eaters, and egg eaters) should be conducted to reveal the relative importance of competing functional, developmental, and genetic factors influencing morphological integration and their micro- and macroevolutionary consequences.

AUTHOR CONTRIBUTIONS

DR contributed to the data acquisition, analysis, interpretation of the results, and writing and editing. DP and CR contributed to the

interpretation and discussion of the results, as well as the review and edits of the manuscript. MS conceived the study, generated the scans, helped in the analyses and the interpretation of results, and reviewed the manuscript.

ACKNOWLEDGMENTS

We thank the herpetological collections staff of the American Museum of Natural History: D. Kizirian, D. Dickey, M. Arnold, and especially L. Vonnahme, but also A. Resetar (Field Museum of Natural History), E. Ely, and L. Scheinberg (California Academy of Sciences) for their help and patience in carefully choosing specimens that fit our study and quickly processing specimen loans. Another special thanks to M. H. Chase and A. Smith from the Microscopy and Imaging and Facility who did all the CT scanning involved in this study. The authors greatly appreciate insightful comments by S. Hellert that improved earlier versions of this manuscript. We thank the National Science Foundation REU program and the Fyssen Foundation for partly funding this research.

DATA ARCHIVING

A 3D landmark file (TPS format) with the average landmark configuration for each species is available in a Dryad repository (<https://doi.org/10.5061/dryad.rbnzs7h9m>).

CONFLICT OF INTEREST

The authors declare no conflict of interest.

LITERATURE CITED

- Adams, D. C. 1999. Methods for shape analysis of landmark data from articulated structures. *Evol. Ecol. Res.* 1:959–970.
- . 2004. Character displacement via aggressive interference in Appalachian salamanders. *Ecology* 85:2664–2670.
- . 2014. A generalized K statistic for estimating phylogenetic signal from shape and other high-dimensional multivariate data. *Syst. Biol.* 63:685–697.
- . 2016. Evaluating modularity in morphometric data: challenges with the RV coefficient and a new test measure. *Methods Ecol. Evol.* 7:565–572.
- Adams, D. C., and E. Otárola-Castillo. 2013. geomorph: an R package for the collection and analysis of geometric morphometric shape data. *Methods Ecol. Evol.* 4:393–399.
- Adams, D. C., and F. J. Rohlf. 2000. Ecological character displacement in *Plethodon*: biomechanical differences found from a geometric morphometric study. *Proc. Natl. Acad. Sci.* 97:4106–4111.
- Adams, D. C., and M. L. Collyer. 2016. On the comparison of the strength of morphological integration across morphometric datasets. *Evolution* 70:2623–2631.
- . 2018. Multivariate phylogenetic comparative methods: evaluations, comparisons, and recommendations. *Syst. Biol.* 67:14–31.
- . 2019. Comparing the strength of modular signal, and evaluating alternative modular hypotheses, using covariance ratio effect sizes with morphometric data. *Evolution* 73:2352–2367.
- Adams, D. C., and R. N. Felice. 2014. Assessing trait covariation and morphological integration on phylogenies using evolutionary covariance matrices. *PLoS One* 9:e94335.
- Adams, D. C., F. J. Rohlf, and D. E. Slice. 2004. Geometric morphometrics: ten years of progress following the ‘revolution’. *Ital. J. Zool.* 71:5–16.
- . 2013. A field comes of age: geometric morphometrics in the 21st century. *Hystrix* 24:7.
- Andjelković, M., L. Tomović, and A. Ivanović. 2016. Variation in skull size and shape of two snake species (*Natrix natrix* and *Natrix tessellata*). *Zoomorphology* 135:243–253.
- . 2017. Morphological integration of the kinetic skull in *Natrix* snakes. *J. Zool.* 303:188–198.
- Atchley, W. R., and B. K. Hall. 1991. A model for development and evolution of complex morphological structures. *Biol. Rev.* 66:101–157.
- Arlegi, M., C. Veschambre-Couture, and A. Gómez-Olivencia. 2020. Evolutionary selection and morphological integration in the vertebral column of modern humans. *Am. J. Phys. Anthropol.* 171:17–36.
- Bardua, C., R. N. Felice, A. Watanabe, A. C. Fabre, and A. Goswami. 2019a. A practical guide to sliding and surface semilandmarks in morphometric analyses. *Integr. Comp. Biol.* 1:obz016.
- Bardua, C., M. Wilkinson, D. J. Gower, E. Sherratt, and A. Goswami. 2019b. Morphological evolution and modularity of the caecilian skull. *BMC Evol. Biol.* 19:30.
- Bardua, C., A. C. Fabre, M. Bon, K. Das, E. L. Stanley, D. C. Blackburn, and A. Goswami. 2020. Evolutionary integration of the frog cranium. *Evolution* 74:1200–1215.
- Bell, E., B. Andres, and A. Goswami. 2011. Integration and dissociation of limb elements in flying vertebrates: a comparison of pterosaurs, birds and bats. *J. Evol. Biol.* 24:2586–2599.
- Boltz, R. E., and R. F. Ewer. 1964. The functional anatomy of the head of the puff adder, *Bitis arietans* (Merr.). *J. Morphol.* 114:83–105.
- Bon, M., C. Bardua, A. Goswami, and A. C. Fabre. 2020. Cranial integration in the fire salamander, *Salamandra salamandra* (Caudata: Salamandridae). *Biol. J. Linn. Soc.* 130:178–194.
- Boughner, J. C., M. Buchtová, K. Fu, V. Diewert, B. Hallgrímsson, and J. M. Richman. 2007. Embryonic development of *Python sebae*–I: staging criteria and macroscopic skeletal morphogenesis of the head and limbs. *Zoology* 110:212–230.
- Caldwell, M. W. 2019. The origin of snakes: morphology and the fossil record. Pp. 1–326. CRC Press, Boca Raton, FL. <https://doi.org/10.1201/9781315118819>.
- Cheverud, J. M. 1984. Quantitative genetics and developmental constraints on evolution by selection. *J. Theor. Biol.* 110:155–171.
- . 1996. Developmental integration and the evolution of pleiotropy. *Am. Zool.* 36:44–50.
- Collyer, M. L., M. A. Davis, and D. C. Adams. 2020. Making heads or tails of combined landmark configurations in geometric morphometric data. *Evol. Biol.* 47:193–204.
- Cundall, D. 1983. Activity of head muscles during feeding by snakes: a comparative study. *Am. Zool.* 23:383–396.
- Cundall, D., and H. W. Greene. 2000. Feeding in snakes. *Feeding*. Pp. 293–333 in K. Schwenk, ed. Academic Press, Amsterdam, the Netherlands. <https://doi.org/10.1016/B978-012632590-4/50010-1>.
- Davis, M. A., M. R. Douglas, M. L. Collyer, and M. E. Douglas. 2016. Deconstructing a species-complex: geometric morphometric and molecular analyses define species in the Western Rattlesnake (*Crotalus viridis*). *PLoS One* 11:e0146166.
- Deufel, A., and D. Cundall. 2003. Feeding in *Atractaspis* (Serpentes: Atractaspididae): a study in conflicting functional constraints. *Zoology* 106:43–61.
- dos Santos, M. M., F. M. da Silva, E. Hingst-Zaher, F. A. Machado, H. E. D. Zaher, and A. L. da Costa Prudente. 2017. Cranial adaptations for feeding on snails in species of *Sibynomorphus* (Dipsadidae: Dipsadinae). *Zoology* 120:24–30.
- Dumont, M., C. E. Wall, L. Botton-Divet, A. Goswami, S. Peigné, and A. C. Fabre. 2016. Do functional demands associated with locomotor habitat, diet, and activity pattern drive skull shape evolution in musteloid carnivorans? *Biol. J. Linn. Soc.* 117:858–878.

- Esquerré, D., E. Sherratt, and J. S. Keogh. 2017. Evolution of extreme ontogenetic allometric diversity and heterochrony in pythons, a clade of giant and dwarf snakes. *Evolution* 71:2829–2844.
- Fabre, A. C., D. Bickford, M. Segall, and A. Herrel. 2016. The impact of diet, habitat use, and behaviour on head shape evolution in homalopsid snakes. *Biol. J. Linn. Soc.* 118:634–647.
- Fabre, A. C., C. Bardua, M. Bon, J. Clavel, R. N. Felice, J. W. Streicher, J. Bonnel, E. L. Stanley, D. C. Blackburn, and A. Goswami. 2020. Metamorphosis shapes cranial diversity and rate of evolution in salamanders. *Nat. Ecol. Evol.* 4:1129–1140.
- Felice, R. N., and A. Goswami. 2018. Developmental origins of mosaic evolution in the avian cranium. *Proc. Natl. Acad. Sci.* 115:555–560.
- Felice, R. N., M. Randau, and A. Goswami. 2018. A fly in a tube: macroevolutionary expectations for integrated phenotypes. *Evolution* 72:2580–2594.
- Felice, R. N., A. Watanabe, A. R. Cuff, E. Noirault, D. Pol, L. M. Witmer, M. A. Norell, P. M. O'Connor, and A. Goswami. 2019. Evolutionary integration and modularity in the archosaur cranium. *Integr. Comp. Biol.* 59:371–382.
- Goswami, A. 2006. Cranial modularity shifts during mammalian evolution. *Am. Nat.* 168:270–280.
- Goswami, A., and P. D. Polly. 2010a. Methods for studying morphological integration and modularity. *Paleontol. Soc. Pap.* 16:213–243.
- . 2010b. The influence of modularity on cranial morphological disparity in Carnivora and Primates (Mammalia). *PLoS One* 5:e9517.
- Goswami, A., J. B. Smaers, C. Soligo, and P. D. Polly. 2014. The macroevolutionary consequences of phenotypic integration: from development to deep time. *Philos. Trans. R. Soc.* 369:20130254.
- Goswami, A., A. Watanabe, R. N. Felice, C. Bardua, A. C. Fabre, and P. D. Polly. 2019. High-density morphometric analysis of shape and integration: the good, the bad, and the not-really-a-problem. *Integr. Comp. Biol.* 59:669–683.
- Gunz, P., P. Mitteroecker, and F. L. Bookstein. 2005. Semilandmarks in Three Dimensions. *Modern Morphometrics in Physical Anthropology*. Pp. 73–98 in D. E. Slice, ed. *Developments in Primatology: Progress and Prospects*. Springer, Boston, MA. https://doi.org/10.1007/0-387-27614-9_3.
- Gunz, P., and P. Mitteroecker. 2013. Semilandmarks: a method for quantifying curves and surfaces. *Hystrix* 24:103–109.
- Hallgrímsson, B., K. Willmore, and B. K. Hall. 2002. Canalization, developmental stability, and morphological integration in primate limbs. *Am. J. Phys. Anthropol.* 119:131–158.
- Hallgrímsson, B., H. Jamniczky, N. M. Young, C. Rolian, T. E. Parsons, J. C. Boughner, and R. S. Marcucio. 2009. Deciphering the palimpsest: studying the relationship between morphological integration and phenotypic covariation. *Evol. Biol.* 36:355–376.
- Hampton, P. M. 2011. Comparison of cranial form and function in association with diet in natricine snakes. *J. Morphol.* 272:1435–1443.
- Jackson, K. 2003. The evolution of venom-delivery systems in snakes. *Zool. J. Linn. Soc.* 137:337–354.
- Jayne, B. C., H. K. Voris, and P. K. L. Ng. 2002. Snake circumvents constraints on prey size. *Nature* 418:143–143.
- . 2018. How big is too big? Using crustacean-eating snakes (Homalopsidae) to test how anatomy and behaviour affect prey size and feeding performance. *Biol. J. Linn. Soc.* 123:636–650.
- Johnston, P. 2014. Homology of the jaw muscles in lizards and snakes—a solution from a comparative gnathostome approach. *Anat. Rec.* 297:574–585.
- Jones, K. E., L. Benitez, K. D. Angielczyk, and S. E. Pierce. 2018. Adaptation and constraint in the evolution of the mammalian backbone. *BMC Evol. Biol.* 18:1–13.
- Jones, K. E., S. Gonzalez, K. D. Angielczyk, and S. E. Pierce. 2020. Regionalization of the axial skeleton predates functional adaptation in the forerunners of mammals. *Nat. Ecol. Evol.* 4:470–478.
- Kardong, K. V. 1977. Kinesis of the jaw apparatus during swallowing in the cottonmouth snake, *Agkistrodon piscivorus*. *Copeia* 1977:338–348.
- . 1979. ‘Protovipers’ and the evolution of snake fangs. *Evolution* 33:433–443.
- Khannoob, E. R., and S. E. Evans. 2015. The development of the skull of the Egyptian cobra *Naja h. haje* (Squamata: Serpentes: Elapidae). *PLoS One* 10:e0122185.
- Klaczko, J., E. Sherratt, and E. Z. Setz. 2016. Are diet preferences associated to skulls shape diversification in xenodontine snakes? *PLoS One* 11:e0148375.
- Klingenberg, C. P. 2008. Morphological integration and developmental modularity. *Annu. Rev. Ecol. Evol. Syst.* 39:115–132.
- . 2014. Studying morphological integration and modularity at multiple levels: concepts and analysis. *Philos. Trans. R. Soc.* 369:20130249.
- Kojima, Y., I. Fukuyama, T. Kurita, M. Y. B. Hossman, and K. Nishikawa. 2020. Mandibular sawing in a snail-eating snake. *Sci. Rep.* 10:1–5.
- Lebrun, R., and M. J. Orliac. 2017. MorphoMuseuM: an online platform for publication and storage of virtual specimens. *Paleontol. Soc. Pap.* 22:183–195.
- Martín-Serra, A., B. Figueirido, and P. Palmqvist. 2020. Changing modular patterns in the carnivoran pelvic girdle. *J. Mamm. Evol.* 27:237–243.
- Marshall, A. F., C. Bardua, D. J. Gower, M. Wilkinson, E. Sherratt, and A. Goswami. 2019. High-density three-dimensional morphometric analyses support conserved static (intraspecific) modularity in caecilian (Amphibia: Gymnophiona) crania. *Biol. J. Linn. Soc.* 126:721–742.
- Melo, D., A. Porto, J. M. Cheverud, and G. Marroig. 2016. Modularity: genes, development, and evolution. *Annu. Rev. Ecol. Evol. Syst.* 47:463–486.
- Murphy, J. C. 2012. Marine invasions by non-sea snakes, with thoughts on terrestrial–aquatic–marine transitions. *Integr. Comp. Biol.* 52:217–226.
- Mushinsky, H. R., J. J. Hebrard, and D. S. Vodopich. 1982. Ontogeny of water snake foraging ecology. *Ecology* 63:1624–1629.
- Murta-Fonseca, R. A., A. Machado, R. T. Lopes, and D. S. Fernandes. 2019. Sexual dimorphism in *Xenodon neuwiedi* skull revealed by geometric morphometrics (Serpentes; Dipsadidae). *Amphibia-Reptilia* 40:461–474.
- Moon, B. R., D. A. Penning, M. Segall, and A. Herrel. 2019. Feeding in Snakes: form, function, and evolution of the feeding system. Pp. 527–574 in V. Belsand I. Whishaw, eds. *Feeding in vertebrates*. Springer, Cham, Switzerland.
- Mori, A., and S. E. Vincent. 2008. An integrative approach to specialization: relationships among feeding morphology, mechanics, behaviour, performance and diet in two syntopic snakes. *J. Zool.* 275:47–56.
- Navalón, G., J. Marugán-Lobón, J. A. Bright, C. R. Cooney, and E. J. Rayfield. 2020. The consequences of craniofacial integration for the adaptive radiations of Darwin’s finches and Hawaiian honeycreepers. *Nat. Ecol. Evol.* 4:270–278.
- Olson, E. C., and R. L. Miller. 1958. *Morphological integration*. Pp. 1–376. University of Chicago Press, Chicago.
- Palci, A., M. S. Lee, and M. N. Hutchinson. 2016. Patterns of postnatal ontogeny of the skull and lower jaw of snakes as revealed by micro-CT scan data and three-dimensional geometric morphometrics. *J. Anat.* 229:723–754.
- Palci, A., M. W. Caldwell, M. N. Hutchinson, T. Konishi, and M. S. Lee. 2020. The morphological diversity of the quadrate bone in squamate

- reptiles as revealed by high-resolution computed tomography and geometric morphometrics. *J. Anat.* 236:210–227.
- Pavlicev, M., J. M. Cheverud, and G. P. Wagner. 2009. Measuring morphological integration using eigenvalue variance. *Evol. Biol.* 36:157–170.
- Polachowski, K. M., and I. Werneburg. 2013. Late embryos and bony skull development in *Bothropoides jararaca* (Serpentes, Viperidae). *Zoology* 116:36–63.
- Pyron, R. A., and F. T. Burbrink. 2014. Early origin of viviparity and multiple reversions to oviparity in squamate reptiles. *Ecol. Lett.* 17:13–21.
- Raff, R. A. 1996. The shape of life: genes, development, and the evolution of animal form. Pp. 1–544. University of Chicago Press, Chicago.
- Randau, M., and A. Goswami. 2017a. Unravelling intravertebral integration, modularity and disparity in Felidae (Mammalia). *Evol. Dev.* 19:85–95.
- . 2017b. Morphological modularity in the vertebral column of Felidae (Mammalia, Carnivora). *BMC Evol. Biol.* 17:133.
- . 2018. Shape covariation (or the lack thereof) between vertebrae and other skeletal traits in felids: the whole is not always greater than the sum of parts. *Evol. Biol.* 45:196–210.
- Revell, L. J. 2009. Size-correction and principal components for interspecific comparative studies. *Evolution* 63:3258–3268.
- Rohlf, F. J., and D. Slice. 1990. Extensions of the Procrustes method for the optimal superimposition of landmarks. *Syst. Biol.* 39:40–59.
- Rohlf, F. J., and M. Corti. 2000. Use of two-block partial least-squares to study covariation in shape. *Syst. Biol.* 49:740–753.
- Savitzky, A. H. 1983. Coadapted character complexes among snakes: fossoriality, piscivory, and durophagy. *Am. Zool.* 23:397–409.
- Scanferla, A. 2016. Postnatal ontogeny and the evolution of macrostomia in snakes. *R. Soc. Open Sci.* 3:160612.
- Schlager, S. 2017. Morpho and Rvecg—shape analysis in R: R-packages for geometric morphometrics, shape analysis and surface manipulations. Pp. 217–256 in G. Zheng, S. Li, and G. Székely, eds. Statistical shape and deformation analysis. Academic Press, Cambridge, MA.
- Sherratt, E., K. L. Sanders, A. Watson, M. N. Hutchinson, M. S. Lee, and A. Palci. 2019. Heterochronic shifts mediate ecomorphological convergence in skull shape of microcephalic sea snakes. *Integr. Comp. Biol.* 59:616–624.
- Segall, M., R. Cornette, A. C. Fabre, R. Godoy-Diana, and A. Herrel. 2016. Does aquatic foraging impact head shape evolution in snakes? *Proc. R. Soc.* 283:20161645.
- Segall, M., A. Herrel, and R. Godoy-Diana. 2019. Hydrodynamics of frontal striking in aquatic snakes: drag, added mass, and the possible consequences for prey capture success. *Bioinspiration & Biomimetics*. 14(3):036005. <https://doi.org/10.1088/1748-3190/ab0316>.
- Segall, M., R. Cornette, R. Godoy-Diana, and A. Herrel. 2020. Exploring the functional meaning of head shape disparity in aquatic snakes. *Ecol. Evol.* 10:6993–7005.
- Sheverdyukova, H. V. 2019. Development of the Osteocranum in *Natrix natrix* (Serpentes, Colubridae) Embryogenesis II: development of the jaws, palatal complex and associated bones. *Acta Zool.* 100:282–291.
- Silva, F. M., A. L. D. C. Prudente, F. A. Machado, M. M. Santos, H. Zaher, and E. Hingst-Zaher. 2018. Aquatic adaptations in a Neotropical coral snake: a study of morphological convergence. *J. Zool. Syst. Evol.* 56:382–394.
- Souto, N. M., R. A. Murta-Fonseca, A. S. Machado, R. T. Lopes, and D. S. Fernandes. 2019. Snakes as a model for measuring skull preparation errors in geometric morphometrics. *J. Zool.* 309:12–21.
- Uetz, P., S. Cherikh, G. Shea, I. Ineich, P. D. Campbell, I. V. Doronin, J. Rosado, A. Wynn, K. Tighe, R. Mcdiarmid, et al. 2019. A global catalog of primary reptile type specimens. *Zootaxa* 4695:438–450.
- Vidal-García, M., and J. S. Keogh. 2017. Phylogenetic conservatism in skulls and evolutionary lability in limbs—morphological evolution across an ancient frog radiation is shaped by diet, locomotion and burrowing. *BMC Evol. Biol.* 17:1–15.
- Vidal-García, M., L. Bandara, and J. S. Keogh. 2018. ShapeRotator: an R tool for standardized rigid rotations of articulated three-dimensional structures with application for geometric morphometrics. *Ecol. Evol.* 8:4669–4675.
- Vincent, S. E., B. R. Moon, A. Herrel, and N. J. Kley. 2007. Are ontogenetic shifts in diet linked to shifts in feeding mechanics? Scaling of the feeding apparatus in the banded watersnake *Nerodia fasciata*. *J. Exp. Biol.* 210:2057–2069.
- Wagner, G. P., and L. Altenberg. 1996. Perspective: complex adaptations and the evolution of evolvability. *Evolution* 50:967–976.
- Wagner, G. P., M. Pavlicev, and J. M. Cheverud. 2007. The road to modularity. *Nat. Rev. Genet.* 8:921–931.
- Wainwright, P. C., and B. A. Richard. 1995. Predicting patterns of prey use from morphology of fishes. *Environ. Biol. Fishes* 44:97–113.
- Watanabe, A., A. C. Fabre, R. N. Felice, J. A. Maisano, J. Müller, A. Herrel, and A. Goswami. 2019. Ecomorphological diversification in squamates from conserved pattern of cranial integration. *Proc. Natl. Acad. Sci.* 116:14688–14697.
- Werneburg, I., K. M. Polachowski, and M. N. Hutchinson. 2015. Bony skull development in the Argus monitor (Squamata, Varanidae, *Varanus panoptes*) with comments on developmental timing and adult anatomy. *Zoology* 118:255–280.
- Wiley, D. F., N. Amenta, D. A. Alcantara, D. Ghosh, Y. J. Kil, E. Delson, W. Harcourt-Smith, F. J. Rohlf, K. St John, et al. 2005. Evolutionary morphing. Pp. 431–438 in Proceedings of IEEE Visualization 2005 (VIS’05). IEEE, Minneapolis, MN.

Associate Editor: A. Kaliontzopoulou
Handling Editor: M. L. Zelditch

Supporting Information

Additional supporting information may be found online in the Supporting Information section at the end of the article.

Supplementary Table 1. Species and specimens used in this study.

Supplementary Table 2. The influence of allometry, phylogeny, and integration on snake skull bones associated with feeding.

Supplementary Table 3. Explanations for each alternative hypothesis of modularity.

Supplementary Table 4. The r-PLS values of PLS1 (above diagonal) and p-values (below diagonal) of each 2BPLS analysis.

Supplementary Table 5. The z-PLS values of PLS1 (above diagonal) and p-values (below diagonal) of each 2BPLS analysis.

Supplementary Table 6. a. Alternative hypotheses of modularity and their support, measured as phylogenetic-corrected ZCR, for both common and local superimposition procedures.

Supplementary Figure 1. The bones analyzed in this article (middle two skulls) and their respective landmark configurations.

Supplementary Figure 2. Principal component morphospace from a common superimposition (GPAAll) of individual specimens of three homalopsid snakes: *Erpeton tentaculatum* (green), *Fordonia leucobalia* (blue), and *Cerberus rynchops* (orange).

Supplementary Figure 3. Morphospace of the first two principal components of the dentary (above), and axes of shape variation along the first two principal components in lateral view (below).

Supplementary Figure 4. Morphospace of the first two principal components of the compound (above), and axes of shape variation along the first two principal components in lateral view (below).

Supplementary Figure 5. Morphospace of the first two principal components of the quadrate (above), and axes of shape variation along the first two principal components in lateral view (below).

Supplementary Figure 6. Morphospace of the first two principal components of the supratemporal (above), and axes of shape variation along the first two principal components in lateral view (below).

Supplementary Figure 7. Morphospace of the first two principal components of the pterygoid (above), and axes of shape variation along the first two principal components in dorsal view (below).

Supplementary Figure 8. Morphospace of the first two principal components of the ectopterygoid (above), and axes of shape variation along the first two principal components in dorsal view (below).

Supplementary Figure 9. Morphospace of the first two principal components of the palatine (above), and axes of shape variation along the first two principal components in dorsal view (below).

Supplementary Figure 10. Morphospace of the first two principal components of the maxilla (above), and axes of shape variation along the first two principal components in dorsal view (below).

Supplementary Figure 11. (Above) Principal component analysis morphospace of landmark configurations generated by the Iterative Rearticulations (Method 1, a.) and Superimposed Centroids (Method 2, b.).

Supplementary Figure 12. Pairwise effect sizes of alternative hypotheses of modularity of the common superimposition (a.) and local superimposition (b.) datasets.